Appendix A

A.1 Cross-section Ratio, R_{32}

Table A.1: Differential cross-sections ($\times 10^{-3}$(pb/GeV)) and the cross-section ratio R_{32} at detector level in each bin of $H_{\mathrm{T},2}/2$, along with statistical uncertainty (in %).

Bin	2-jet cross-section	Stat. unc.	3-jet cross-section	Stat. unc.	Ratio R_{32}	Stat. unc.
300 - 330	29772.726	0.211	2640.629	0.707	0.089	$^{+0.665}_{-0.661}$
330 - 360	16792.917	0.231	1773.485	0.704	0.106	$^{+0.523}_{-0.521}$
360 - 390	9889.326	0.182	1176.544	0.526	0.119	$^{+0.485}_{-0.483}$
390 - 420	5976.777	0.179	778.034	0.492	0.130	$^{+0.206}_{-0.206}$
420 - 450	3731.760	0.067	522.624	0.180	0.140	$^{+0.167}_{-0.167}$
450 - 480	2398.741	0.084	357.622	0.217	0.149	$^{+0.201}_{-0.200}$
480 - 510	1570.192	0.104	246.051	0.262	0.157	$^{+0.241}_{-0.241}$
510 - 540	1048.665	0.127	171.080	0.314	0.163	$^{+0.288}_{-0.287}$
540 - 570	713.042	0.154	119.566	0.376	0.168	$^{+0.344}_{-0.343}$
570 - 600	490.776	0.186	84.798	0.447	0.173	$^{+0.407}_{-0.406}$
600 - 640	325.046	0.198	57.463	0.470	0.177	$^{+0.427}_{-0.426}$
640 - 680	205.727	0.248	37.282	0.583	0.181	$^{+0.529}_{-0.527}$
680 - 720	133.674	0.308	24.859	0.714	0.186	$^{+0.646}_{-0.643}$
720 - 760	87.911	0.380	16.560	0.875	0.188	$^{+0.791}_{-0.786}$
760 - 800	58.657	0.465	11.056	1.071	0.188	$^{+0.968}_{-0.961}$
800 - 850	38.106	0.516	7.318	1.178	0.192	$^{+1.063}_{-1.054}$
850 - 900	23.587	0.656	4.600	1.485	0.195	$^{+1.339}_{-1.326}$
900 - 950	15.130	0.819	2.896	1.872	0.191	$^{+1.694}_{-1.672}$
950 - 1000	9.696	1.023	1.812	2.366	0.187	$^{+2.151}_{-2.116}$
1000 - 1060	6.026	1.185	1.186	2.670	0.197	$^{+2.414}_{-2.371}$
1060 - 1120	3.668	1.518	0.716	3.436	0.195	$^{+3.118}_{-3.046}$
1120 - 1180	2.327	1.906	0.437	4.398	0.188	$^{+4.024}_{-3.903}$
1180 - 1250	1.419	2.260	0.265	5.227	0.187	$^{+4.798}_{-4.627}$
1250 - 1320	0.853	2.915	0.165	6.623	0.194	$^{+6.080}_{-5.811}$
1320 - 1390	0.477	3.898	0.080	9.492	0.169	$^{+8.951}_{-8.355}$
1390 - 1460	0.263	5.249	0.042	13.131	0.160	$^{+12.619}_{-11.449}$
1460 - 1530	0.192	6.143	0.029	15.811	0.151	$^{+15.437}_{-13.698}$
1530 - 1600	0.104	8.362	0.021	18.570	0.203	$^{+17.571}_{-15.536}$
1600 - 1680	0.060	10.314	0.009	26.726	0.149	$^{+27.132}_{-22.170}$

A.2 Individual Sources of Jet Energy Correction Uncertainties

The sources of JEC considered in the current measurements are : AbsoluteStat, AbsoluteScale, AbsoluteFlavMap, AbsoluteMPFBias, Fragmentation, SinglePionECAL, SinglePionHCAL, FlavorQCD, RelativeJEREC1, RelativeJEREC2, RelativeJERHF, RelativePtBB, RelativePtEC1, RelativePtEC2, RelativePtHF, RelativeFSR, RelativeStatFSR, RelativeStatEC2, RelativeStatHF, PileUpDataMC, PileUpPtRef, PileUpPtBB, PileUpPtEC1, PileUpPtEC2 and PileUpPtHF. The AbsoluteFlavMap uncertainty is exactly zero for the 8 TeV and can be ignored. For the four sources : RelativeJERHF, RelativePtHF, RelativeStatHF, PileUpPtHF, the JEC uncertainty is exactly zero because of $|y| < 2.5$ cut used in the analysis. So only 20 sources contribute to the total JEC uncertainty.

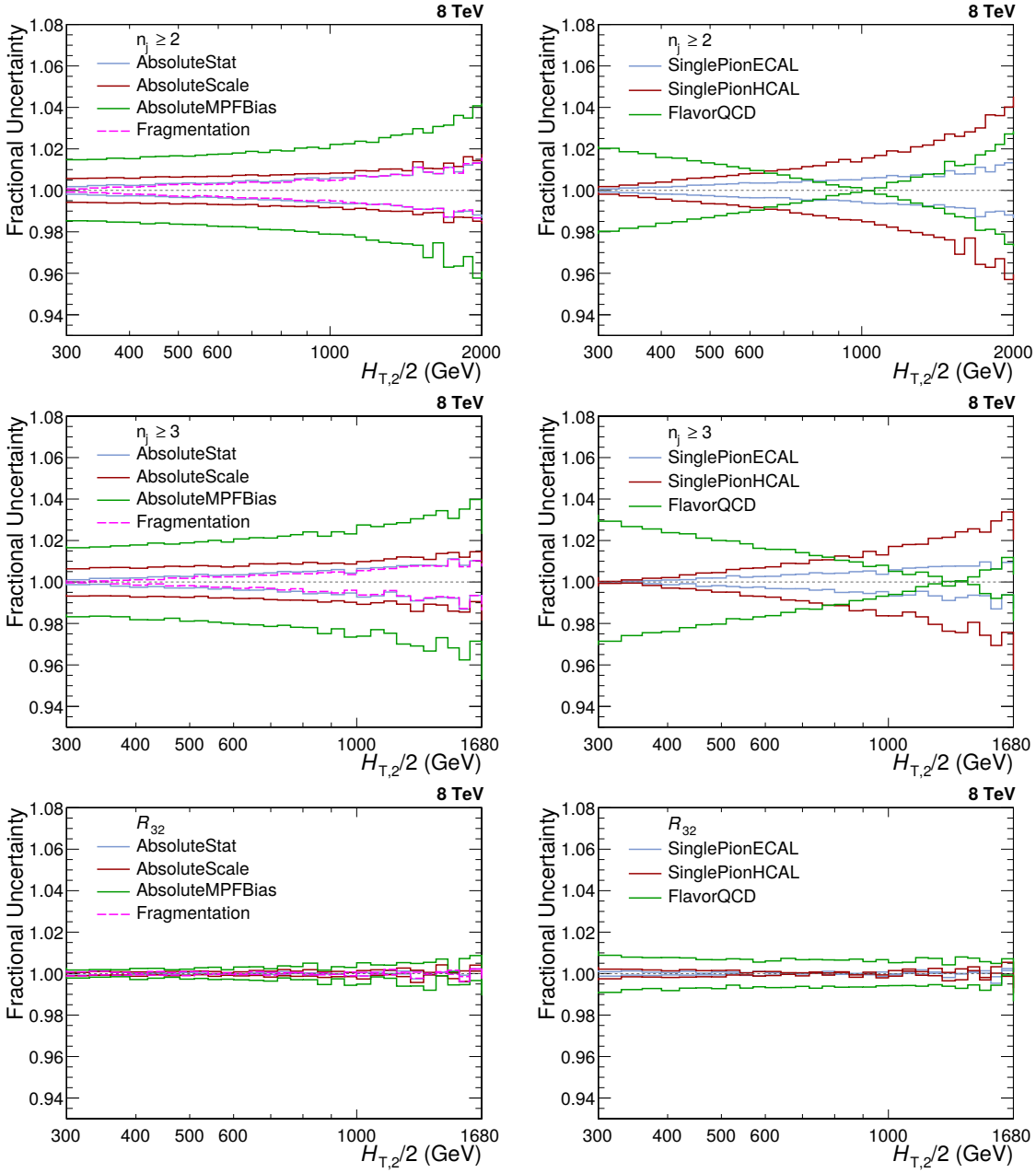

Figure A.1: The fractional jet energy correction (JEC) uncertainties from individual sources are shown for inclusive 2-jet (top) and 3-jet (middle) events cross-sections and the cross-section ratio R_{32} (bottom). On left, JEC uncertainties are evaluated from AbsoluteStat (blue), AbsoluteScale (red), AbsoluteMPFBias (green) and Fragmentation (pink) sources whereas on right, these are evaluated from SinglePionECAL (blue), SinglePionHCAL (red) and FlavorQCD (green) sources.

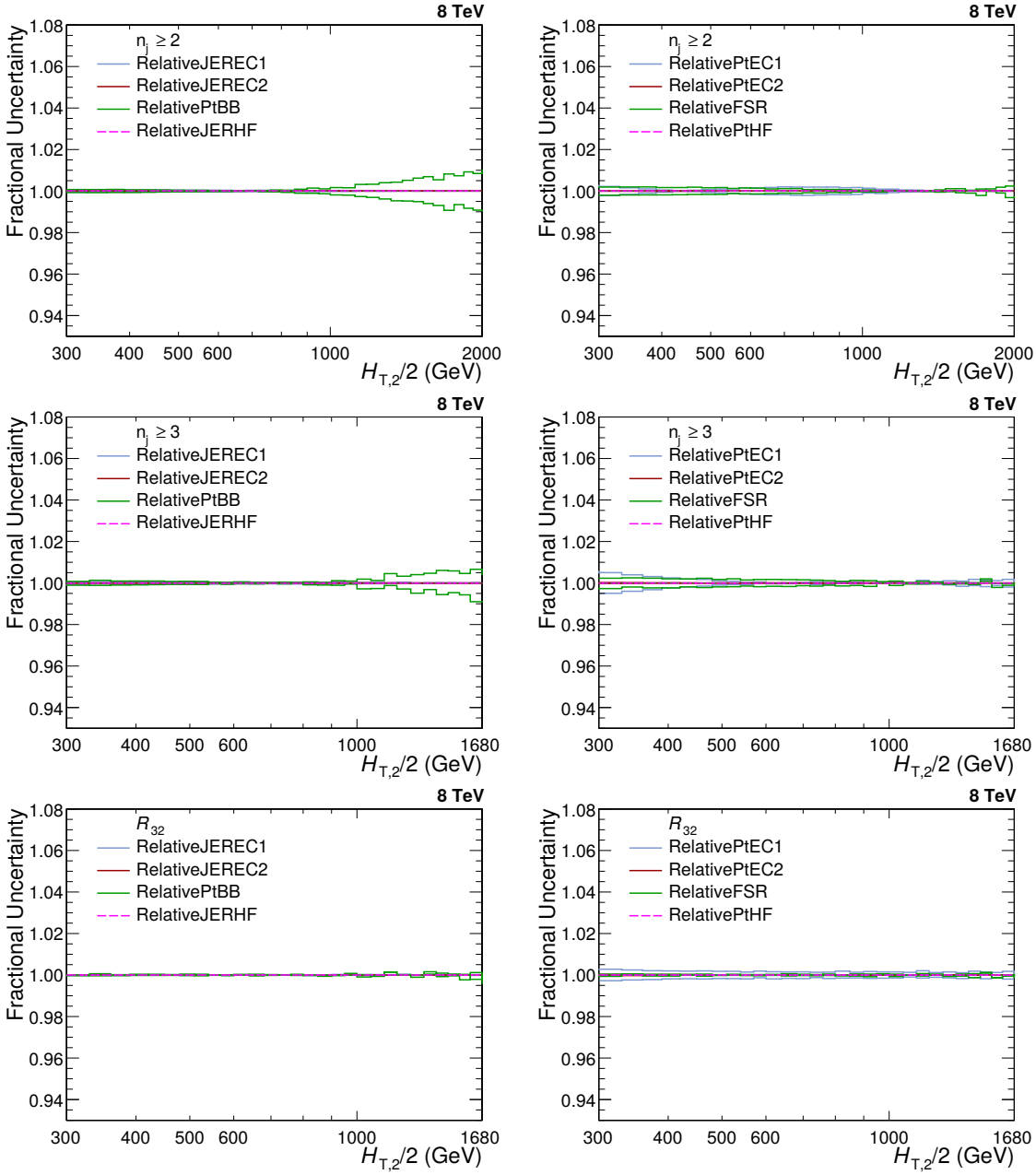

Figure A.2: The fractional jet energy correction (JEC) uncertainties from individual sources are shown for inclusive 2-jet (top) and 3-jet (middle) events cross-sections and the cross-section ratio R_{32} (bottom). On left, JEC uncertainties are evaluated from RelativeJEREC1 (blue), RelativeJEREC2 (red), RelativePtBB (green) and RelativeJERHF (pink) sources whereas on right, these are evaluated from RelativePtEC1 (blue), RelativePtEC2 (red), RelativePFSR (green) and RelativePtHF (pink) sources.

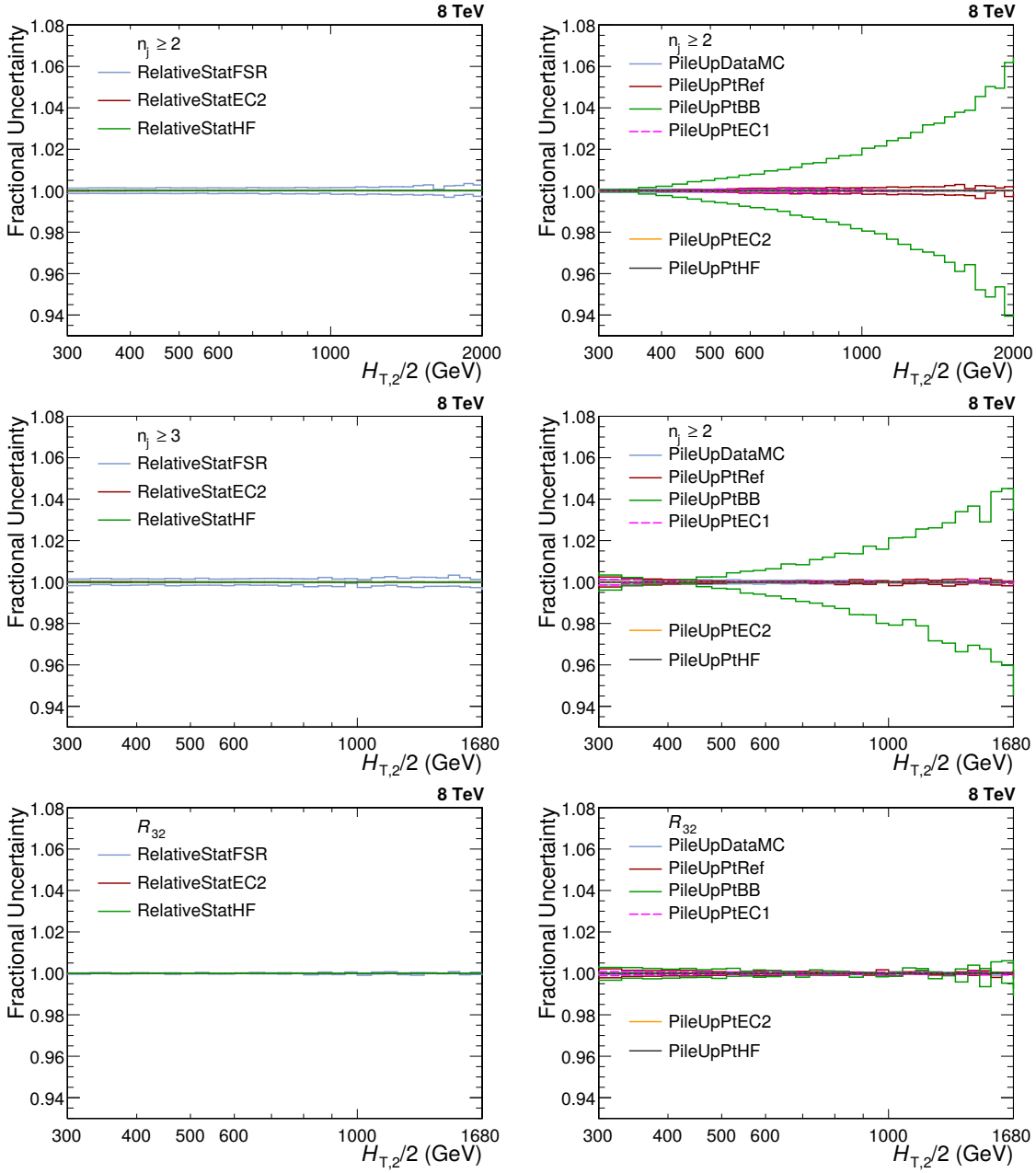

Figure A.3: The fractional jet energy correction (JEC) uncertainties from individual sources are shown for inclusive 2-jet (top) and 3-jet (middle) events cross-sections and the cross-section ratio R_{32} (bottom). On left, JEC uncertainties are evaluated from RelativeStatFSR (blue), RelativeStatEC2 (red) and RelativeStatHF (green) sources whereas on right, these are evaluated from PileUpDataMC (blue), PileUpPtRef (red), PileUpPtBB (green), PileUpPtEC1 (pink), PileUpPtEC2 (orange) and PileUpPtHF (black) sources.

A.3 Experimental Uncertainties

Table A.2: Experimental uncertainties (in %), from all sources as well as the total uncertainty, affecting the cross-section measurement in each bin of $H_{\mathrm{T},2}/2$ for inclusive 2-jet events.

Bin	Statistical	JEC	Unfolding	Lumi	Residual	Total
300 - 330	0.242	$^{+2.612}_{-2.565}$	$^{+0.948}_{-0.928}$	2.6	1.0	$^{+3.942}_{-3.906}$
330 - 360	0.258	$^{+2.507}_{-2.473}$	$^{+0.976}_{-0.969}$	2.6	1.0	$^{+3.882}_{-3.858}$
360 - 390	0.202	$^{+2.504}_{-2.465}$	$^{+0.779}_{-0.783}$	2.6	1.0	$^{+3.831}_{-3.807}$
390 - 420	0.193	$^{+2.363}_{-2.381}$	$^{+0.905}_{-0.904}$	2.6	1.0	$^{+3.768}_{-3.780}$
420 - 450	0.084	$^{+2.448}_{-2.422}$	$^{+0.904}_{-0.895}$	2.6	1.0	$^{+3.818}_{-3.799}$
450 - 480	0.096	$^{+2.440}_{-2.352}$	$^{+0.797}_{-0.795}$	2.6	1.0	$^{+3.789}_{-3.733}$
480 - 510	0.107	$^{+2.427}_{-2.406}$	$^{+0.728}_{-0.715}$	2.6	1.0	$^{+3.767}_{-3.751}$
510 - 540	0.128	$^{+2.425}_{-2.395}$	$^{+0.835}_{-0.862}$	2.6	1.0	$^{+3.789}_{-3.775}$
540 - 570	0.154	$^{+2.425}_{-2.376}$	$^{+0.687}_{-0.674}$	2.6	1.0	$^{+3.760}_{-3.726}$
570 - 600	0.180	$^{+2.497}_{-2.474}$	$^{+0.839}_{-0.827}$	2.6	1.0	$^{+3.838}_{-3.820}$
600 - 640	0.209	$^{+2.495}_{-2.491}$	$^{+0.744}_{-0.743}$	2.6	1.0	$^{+3.819}_{-3.816}$
640 - 680	0.264	$^{+2.582}_{-2.545}$	$^{+0.912}_{-0.912}$	2.6	1.0	$^{+3.915}_{-3.891}$
680 - 720	0.320	$^{+2.691}_{-2.574}$	$^{+0.763}_{-0.756}$	2.6	1.0	$^{+3.961}_{-3.880}$
720 - 760	0.387	$^{+2.690}_{-2.755}$	$^{+0.705}_{-0.712}$	2.6	1.0	$^{+3.955}_{-4.001}$
760 - 800	0.465	$^{+2.858}_{-2.846}$	$^{+0.859}_{-0.846}$	2.6	1.0	$^{+4.109}_{-4.098}$
800 - 850	0.548	$^{+2.889}_{-2.913}$	$^{+0.783}_{-0.787}$	2.6	1.0	$^{+4.126}_{-4.143}$
850 - 900	0.698	$^{+3.145}_{-3.102}$	$^{+0.961}_{-0.958}$	2.6	1.0	$^{+4.366}_{-4.334}$
900 - 950	0.847	$^{+3.298}_{-3.233}$	$^{+0.828}_{-0.829}$	2.6	1.0	$^{+4.476}_{-4.429}$
950 - 1000	1.041	$^{+3.291}_{-3.330}$	$^{+0.895}_{-0.872}$	2.6	1.0	$^{+4.525}_{-4.549}$
1000 - 1060	1.268	$^{+3.598}_{-3.569}$	$^{+0.945}_{-0.956}$	2.6	1.0	$^{+4.817}_{-4.798}$
1060 - 1120	1.611	$^{+3.759}_{-3.756}$	$^{+0.970}_{-0.967}$	2.6	1.0	$^{+5.043}_{-5.040}$
1120 - 1180	1.985	$^{+4.154}_{-4.053}$	$^{+1.089}_{-1.080}$	2.6	1.0	$^{+5.490}_{-5.413}$
1180 - 1250	2.406	$^{+4.251}_{-4.313}$	$^{+1.062}_{-1.070}$	2.6	1.0	$^{+5.722}_{-5.770}$
1250 - 1320	3.101	$^{+4.696}_{-4.624}$	$^{+1.151}_{-1.144}$	2.6	1.0	$^{+6.384}_{-6.330}$
1320 - 1390	4.157	$^{+4.934}_{-4.979}$	$^{+1.343}_{-1.341}$	2.6	1.0	$^{+7.155}_{-7.186}$
1390 - 1460	5.270	$^{+5.148}_{-5.104}$	$^{+1.185}_{-1.177}$	2.6	1.0	$^{+7.965}_{-7.936}$
1460 - 1530	6.360	$^{+5.890}_{-5.652}$	$^{+1.405}_{-1.406}$	2.6	1.0	$^{+9.213}_{-9.063}$
1530 - 1600	8.183	$^{+5.924}_{-6.311}$	$^{+1.598}_{-1.590}$	2.6	1.0	$^{+10.601}_{-10.821}$
1600 - 1680	10.630	$^{+5.969}_{-5.655}$	$^{+1.607}_{-1.592}$	2.6	1.0	$^{+12.608}_{-12.461}$
1680 - 1760	13.864	$^{+7.245}_{-7.603}$	$^{+1.821}_{-1.839}$	2.6	1.0	$^{+15.993}_{-16.161}$
1760 - 1840	18.192	$^{+7.781}_{-7.820}$	$^{+1.902}_{-1.906}$	2.6	1.0	$^{+20.071}_{-20.087}$
1840 - 1920	22.612	$^{+7.647}_{-7.537}$	$^{+1.588}_{-1.590}$	2.6	1.0	$^{+24.085}_{-24.050}$
1920 - 2000	29.530	$^{+9.199}_{-9.469}$	$^{+1.511}_{-1.505}$	2.6	1.0	$^{+31.092}_{-31.172}$

Table A.3: Experimental uncertainties (in %), from all sources as well as the total uncertainty, affecting the cross-section measurement in each bin of $H_{\mathrm{T},2}/2$ for inclusive 3-jet events.

Bin	**Statistical**	**JEC**	**Unfolding**	**Lumi**	**Residual**	**Total**
300 - 330	0.796	$^{+3.503}_{-3.475}$	$^{+0.564}_{-0.552}$	2.6	1.0	$^{+4.581}_{-4.558}$
330 - 360	0.781	$^{+3.303}_{-3.186}$	$^{+0.640}_{-0.633}$	2.6	1.0	$^{+4.437}_{-4.350}$
360 - 390	0.583	$^{+3.221}_{-3.094}$	$^{+0.490}_{-0.496}$	2.6	1.0	$^{+4.326}_{-4.233}$
390 - 420	0.531	$^{+3.092}_{-3.149}$	$^{+0.584}_{-0.584}$	2.6	1.0	$^{+4.236}_{-4.278}$
420 - 450	0.224	$^{+3.125}_{-2.996}$	$^{+0.604}_{-0.592}$	2.6	1.0	$^{+4.236}_{-4.140}$
450 - 480	0.248	$^{+2.984}_{-2.890}$	$^{+0.531}_{-0.528}$	2.6	1.0	$^{+4.124}_{-4.056}$
480 - 510	0.269	$^{+2.937}_{-2.963}$	$^{+0.511}_{-0.512}$	2.6	1.0	$^{+4.089}_{-4.108}$
510 - 540	0.318	$^{+3.021}_{-2.797}$	$^{+0.592}_{-0.612}$	2.6	1.0	$^{+4.164}_{-4.007}$
540 - 570	0.375	$^{+2.999}_{-2.935}$	$^{+0.506}_{-0.500}$	2.6	1.0	$^{+4.141}_{-4.094}$
570 - 600	0.434	$^{+2.824}_{-2.906}$	$^{+0.646}_{-0.620}$	2.6	1.0	$^{+4.042}_{-4.096}$
600 - 640	0.497	$^{+2.952}_{-2.956}$	$^{+0.598}_{-0.604}$	2.6	1.0	$^{+4.133}_{-4.136}$
640 - 680	0.617	$^{+3.111}_{-3.001}$	$^{+0.777}_{-0.786}$	2.6	1.0	$^{+4.292}_{-4.215}$
680 - 720	0.739	$^{+3.067}_{-2.984}$	$^{+0.642}_{-0.611}$	2.6	1.0	$^{+4.257}_{-4.194}$
720 - 760	0.895	$^{+3.185}_{-3.111}$	$^{+0.595}_{-0.607}$	2.6	1.0	$^{+4.366}_{-4.313}$
760 - 800	1.068	$^{+3.231}_{-3.166}$	$^{+0.763}_{-0.774}$	2.6	1.0	$^{+4.464}_{-4.419}$
800 - 850	1.250	$^{+3.427}_{-3.295}$	$^{+0.674}_{-0.687}$	2.6	1.0	$^{+4.639}_{-4.544}$
850 - 900	1.578	$^{+3.364}_{-3.540}$	$^{+0.903}_{-0.898}$	2.6	1.0	$^{+4.731}_{-4.857}$
900 - 950	1.961	$^{+3.594}_{-3.524}$	$^{+0.792}_{-0.793}$	2.6	1.0	$^{+5.015}_{-4.965}$
950 - 1000	2.420	$^{+3.603}_{-3.783}$	$^{+0.846}_{-0.843}$	2.6	1.0	$^{+5.226}_{-5.351}$
1000 - 1060	2.844	$^{+4.164}_{-4.116}$	$^{+0.916}_{-0.940}$	2.6	1.0	$^{+5.834}_{-5.803}$
1060 - 1120	3.647	$^{+4.038}_{-3.815}$	$^{+0.963}_{-0.957}$	2.6	1.0	$^{+6.188}_{-6.044}$
1120 - 1180	4.607	$^{+4.278}_{-4.183}$	$^{+1.084}_{-1.087}$	2.6	1.0	$^{+6.961}_{-6.904}$
1180 - 1250	5.532	$^{+4.894}_{-4.771}$	$^{+1.074}_{-1.069}$	2.6	1.0	$^{+7.967}_{-7.891}$
1250 - 1320	7.141	$^{+5.144}_{-5.273}$	$^{+1.222}_{-1.217}$	2.6	1.0	$^{+9.312}_{-9.383}$
1320 - 1390	10.207	$^{+5.542}_{-5.642}$	$^{+1.414}_{-1.428}$	2.6	1.0	$^{+12.027}_{-12.076}$
1390 - 1460	13.831	$^{+5.630}_{-5.265}$	$^{+1.257}_{-1.256}$	2.6	1.0	$^{+15.242}_{-15.111}$
1460 - 1530	15.578	$^{+5.576}_{-5.491}$	$^{+1.546}_{-1.551}$	2.6	1.0	$^{+16.850}_{-16.822}$
1530 - 1600	18.729	$^{+6.409}_{-7.019}$	$^{+1.718}_{-1.716}$	2.6	1.0	$^{+20.063}_{-20.266}$
1600 - 1680	26.465	$^{+7.017}_{-6.255}$	$^{+1.775}_{-1.765}$	2.6	1.0	$^{+27.578}_{-27.393}$

Table A.4: Experimental uncertainties (in %), from all sources as well as the total uncertainty, affecting the measurement of cross-section ratio R_{32}, in each bin of $H_{\mathrm{T},2}/2$.

Bin	**Statistical**	**JEC**	**Unfolding**	**Total**
300 - 330	0.741	$^{+1.059}_{-1.097}$	$^{+0.754}_{-0.751}$	$^{+1.496}_{-1.522}$
330 - 360	0.587	$^{+0.954}_{-0.923}$	$^{+0.685}_{-0.689}$	$^{+1.313}_{-1.292}$
360 - 390	0.519	$^{+0.902}_{-0.855}$	$^{+0.594}_{-0.593}$	$^{+1.199}_{-1.163}$
390 - 420	0.236	$^{+0.907}_{-0.952}$	$^{+0.439}_{-0.438}$	$^{+1.035}_{-1.074}$
420 - 450	0.192	$^{+0.900}_{-0.835}$	$^{+0.360}_{-0.361}$	$^{+0.988}_{-0.930}$
450 - 480	0.209	$^{+0.788}_{-0.802}$	$^{+0.307}_{-0.308}$	$^{+0.872}_{-0.884}$
480 - 510	0.245	$^{+0.795}_{-0.867}$	$^{+0.254}_{-0.235}$	$^{+0.870}_{-0.931}$
510 - 540	0.287	$^{+0.852}_{-0.682}$	$^{+0.264}_{-0.268}$	$^{+0.937}_{-0.787}$
540 - 570	0.326	$^{+0.807}_{-0.803}$	$^{+0.193}_{-0.189}$	$^{+0.891}_{-0.887}$
570 - 600	0.397	$^{+0.656}_{-0.774}$	$^{+0.199}_{-0.219}$	$^{+0.792}_{-0.898}$
600 - 640	0.447	$^{+0.763}_{-0.797}$	$^{+0.150}_{-0.154}$	$^{+0.897}_{-0.926}$
640 - 680	0.573	$^{+0.861}_{-0.781}$	$^{+0.153}_{-0.140}$	$^{+1.045}_{-0.979}$
680 - 720	0.663	$^{+0.766}_{-0.787}$	$^{+0.147}_{-0.164}$	$^{+1.024}_{-1.042}$
720 - 760	0.774	$^{+0.842}_{-0.769}$	$^{+0.118}_{-0.118}$	$^{+1.149}_{-1.097}$
760 - 800	0.970	$^{+0.800}_{-0.729}$	$^{+0.115}_{-0.096}$	$^{+1.263}_{-1.218}$
800 - 850	1.116	$^{+0.873}_{-0.775}$	$^{+0.115}_{-0.104}$	$^{+1.422}_{-1.363}$
850 - 900	1.436	$^{+0.770}_{-0.896}$	$^{+0.069}_{-0.069}$	$^{+1.631}_{-1.694}$
900 - 950	1.716	$^{+0.704}_{-0.752}$	$^{+0.050}_{-0.051}$	$^{+1.855}_{-1.874}$
950 - 1000	2.156	$^{+0.824}_{-0.897}$	$^{+0.089}_{-0.045}$	$^{+2.310}_{-2.336}$
1000 - 1060	2.554	$^{+0.812}_{-0.870}$	$^{+0.045}_{-0.040}$	$^{+2.680}_{-2.698}$
1060 - 1120	3.244	$^{+0.792}_{-0.658}$	$^{+0.018}_{-0.027}$	$^{+3.339}_{-3.310}$
1120 - 1180	4.121	$^{+0.985}_{-0.757}$	$^{+0.025}_{-0.043}$	$^{+4.237}_{-4.191}$
1180 - 1250	4.990	$^{+1.031}_{-0.848}$	$^{+0.023}_{-0.041}$	$^{+5.095}_{-5.062}$
1250 - 1320	6.456	$^{+0.750}_{-1.087}$	$^{+0.079}_{-0.079}$	$^{+6.500}_{-6.548}$
1320 - 1390	8.990	$^{+1.112}_{-1.144}$	$^{+0.080}_{-0.099}$	$^{+9.059}_{-9.063}$
1390 - 1460	12.699	$^{+1.157}_{-0.815}$	$^{+0.076}_{-0.078}$	$^{+12.751}_{-12.725}$
1460 - 1530	13.926	$^{+0.768}_{-1.235}$	$^{+0.143}_{-0.145}$	$^{+13.948}_{-13.981}$
1530 - 1600	16.903	$^{+1.050}_{-1.258}$	$^{+0.120}_{-0.127}$	$^{+16.936}_{-16.950}$
1600 - 1680	28.070	$^{+1.471}_{-0.859}$	$^{+0.178}_{-0.177}$	$^{+28.109}_{-28.084}$

A.4 Theoretical Uncertainties

Table A.5: Theoretical uncertainties (in %), calculated using CT10-NLO PDF set from all sources as well as the total uncertainty, affecting the cross-section measurement in each bin of $H_{\mathrm{T},2}/2$ for inclusive 2-jet events.

Bin	Scale	PDF	NP	Total
300 - 330	$^{+0.942}_{-6.149}$	$^{+3.566}_{-3.090}$	0.825	$^{+3.780}_{-6.931}$
330 - 360	$^{+1.035}_{-6.289}$	$^{+3.906}_{-3.342}$	0.736	$^{+4.107}_{-7.159}$
360 - 390	$^{+1.159}_{-6.438}$	$^{+4.232}_{-3.573}$	0.696	$^{+4.442}_{-7.396}$
390 - 420	$^{+1.220}_{-6.536}$	$^{+4.551}_{-3.794}$	0.723	$^{+4.767}_{-7.592}$
420 - 450	$^{+1.326}_{-6.660}$	$^{+4.857}_{-3.997}$	0.745	$^{+5.089}_{-7.802}$
450 - 480	$^{+1.421}_{-6.776}$	$^{+5.153}_{-4.186}$	0.765	$^{+5.399}_{-8.001}$
480 - 510	$^{+1.512}_{-6.888}$	$^{+5.444}_{-4.365}$	0.782	$^{+5.704}_{-8.192}$
510 - 540	$^{+1.566}_{-6.967}$	$^{+5.721}_{-4.527}$	0.797	$^{+5.984}_{-8.347}$
540 - 570	$^{+1.666}_{-7.082}$	$^{+6.000}_{-4.682}$	0.810	$^{+6.279}_{-8.528}$
570 - 600	$^{+1.731}_{-7.172}$	$^{+6.269}_{-4.825}$	0.822	$^{+6.555}_{-8.683}$
600 - 640	$^{+1.805}_{-7.271}$	$^{+6.597}_{-4.979}$	0.833	$^{+6.890}_{-8.852}$
640 - 680	$^{+1.930}_{-7.416}$	$^{+6.978}_{-5.143}$	0.845	$^{+7.289}_{-9.064}$
680 - 720	$^{+2.007}_{-7.527}$	$^{+7.364}_{-5.295}$	0.856	$^{+7.680}_{-9.243}$
720 - 760	$^{+2.113}_{-7.663}$	$^{+7.749}_{-5.437}$	0.865	$^{+8.078}_{-9.436}$
760 - 800	$^{+2.196}_{-7.781}$	$^{+8.140}_{-5.569}$	0.873	$^{+8.476}_{-9.609}$
800 - 850	$^{+2.323}_{-7.945}$	$^{+8.573}_{-5.706}$	0.881	$^{+8.926}_{-9.822}$
850 - 900	$^{+2.389}_{-8.062}$	$^{+9.082}_{-5.863}$	0.889	$^{+9.433}_{-10.008}$
900 - 950	$^{+2.499}_{-8.227}$	$^{+9.600}_{-6.018}$	0.896	$^{+9.961}_{-10.232}$
950 - 1000	$^{+2.631}_{-8.402}$	$^{+10.134}_{-6.166}$	0.902	$^{+10.509}_{-10.460}$
1000 - 1060	$^{+2.738}_{-8.569}$	$^{+10.747}_{-6.343}$	0.908	$^{+11.127}_{-10.700}$
1060 - 1120	$^{+2.853}_{-8.751}$	$^{+11.431}_{-6.526}$	0.914	$^{+11.817}_{-10.955}$
1120 - 1180	$^{+2.992}_{-8.970}$	$^{+12.183}_{-6.727}$	0.919	$^{+12.579}_{-11.250}$
1180 - 1250	$^{+3.135}_{-9.194}$	$^{+13.019}_{-6.944}$	0.924	$^{+13.423}_{-11.558}$
1250 - 1320	$^{+3.324}_{-9.469}$	$^{+14.004}_{-7.189}$	0.929	$^{+14.423}_{-11.925}$
1320 - 1390	$^{+3.434}_{-9.677}$	$^{+15.080}_{-7.444}$	0.933	$^{+15.494}_{-12.244}$
1390 - 1460	$^{+3.629}_{-9.976}$	$^{+16.223}_{-7.700}$	0.937	$^{+16.650}_{-12.637}$
1460 - 1530	$^{+3.760}_{-10.224}$	$^{+17.505}_{-7.980}$	0.940	$^{+17.929}_{-13.004}$
1530 - 1600	$^{+3.894}_{-10.471}$	$^{+18.891}_{-8.258}$	0.943	$^{+19.311}_{-13.368}$
1600 - 1680	$^{+4.107}_{-10.813}$	$^{+20.496}_{-8.560}$	0.946	$^{+20.925}_{-13.824}$
1680 - 1760	$^{+4.421}_{-11.101}$	$^{+22.481}_{-8.905}$	0.949	$^{+22.931}_{-14.263}$
1760 - 1840	$^{+4.921}_{-11.461}$	$^{+24.654}_{-9.251}$	0.951	$^{+25.158}_{-14.760}$
1840 - 1920	$^{+5.404}_{-11.813}$	$^{+27.143}_{-9.607}$	0.953	$^{+27.692}_{-15.256}$
1920 - 2000	$^{+5.867}_{-12.154}$	$^{+29.986}_{-9.973}$	0.955	$^{+30.570}_{-15.751}$

Table A.6: Theoretical uncertainties (in %), calculated using CT10-NLO PDF set from all sources as well as the total uncertainty, affecting the cross-section measurement in each bin of $H_{\mathrm{T},2}/2$ for inclusive 3-jet events.

Bin	**Scale**	**PDF**	**NP**	**Total**
300 - 330	$^{+0.539}_{-8.294}$	$^{+5.716}_{-4.657}$	1.692	$^{+5.986}_{-9.662}$
330 - 360	$^{+0.550}_{-8.577}$	$^{+5.977}_{-4.779}$	1.516	$^{+6.191}_{-9.935}$
360 - 390	$^{+0.599}_{-8.709}$	$^{+6.187}_{-4.987}$	1.363	$^{+6.363}_{-10.128}$
390 - 420	$^{+0.719}_{-8.948}$	$^{+6.751}_{-5.223}$	1.228	$^{+6.900}_{-10.433}$
420 - 450	$^{+0.799}_{-9.145}$	$^{+7.031}_{-5.395}$	1.110	$^{+7.162}_{-10.676}$
450 - 480	$^{+0.847}_{-9.247}$	$^{+7.404}_{-5.578}$	1.005	$^{+7.520}_{-10.845}$
480 - 510	$^{+0.847}_{-9.294}$	$^{+7.837}_{-5.717}$	0.937	$^{+7.938}_{-10.951}$
510 - 540	$^{+0.922}_{-9.436}$	$^{+8.198}_{-5.884}$	0.921	$^{+8.301}_{-11.158}$
540 - 570	$^{+0.974}_{-9.566}$	$^{+8.529}_{-6.000}$	0.904	$^{+8.632}_{-11.328}$
570 - 600	$^{+1.086}_{-9.786}$	$^{+8.970}_{-6.156}$	0.886	$^{+9.079}_{-11.595}$
600 - 640	$^{+1.107}_{-9.852}$	$^{+9.402}_{-6.297}$	0.866	$^{+9.506}_{-11.724}$
640 - 680	$^{+1.278}_{-10.101}$	$^{+10.310}_{-6.526}$	0.842	$^{+10.423}_{-12.055}$
680 - 720	$^{+1.384}_{-10.342}$	$^{+9.682}_{-6.618}$	0.820	$^{+9.815}_{-12.305}$
720 - 760	$^{+1.415}_{-10.404}$	$^{+11.051}_{-6.826}$	0.798	$^{+11.170}_{-12.469}$
760 - 800	$^{+1.547}_{-10.615}$	$^{+11.565}_{-7.009}$	0.777	$^{+11.694}_{-12.744}$
800 - 850	$^{+1.679}_{-10.804}$	$^{+12.242}_{-7.185}$	0.755	$^{+12.379}_{-12.997}$
850 - 900	$^{+2.085}_{-11.134}$	$^{+13.097}_{-7.461}$	0.731	$^{+13.282}_{-13.422}$
900 - 950	$^{+2.475}_{-11.432}$	$^{+13.889}_{-7.703}$	0.709	$^{+14.125}_{-13.804}$
950 - 1000	$^{+2.655}_{-11.608}$	$^{+14.614}_{-7.915}$	0.688	$^{+14.869}_{-14.066}$
1000 - 1060	$^{+3.025}_{-11.926}$	$^{+15.576}_{-8.173}$	0.667	$^{+15.881}_{-14.473}$
1060 - 1120	$^{+3.299}_{-12.189}$	$^{+14.250}_{-8.441}$	0.645	$^{+14.641}_{-14.840}$
1120 - 1180	$^{+3.741}_{-12.584}$	$^{+17.984}_{-8.787}$	0.625	$^{+18.380}_{-15.361}$
1180 - 1250	$^{+3.969}_{-12.843}$	$^{+19.324}_{-9.127}$	0.625	$^{+19.737}_{-15.768}$
1250 - 1320	$^{+4.663}_{-13.452}$	$^{+21.246}_{-9.517}$	0.642	$^{+21.761}_{-16.490}$
1320 - 1390	$^{+4.878}_{-13.702}$	$^{+22.884}_{-9.899}$	0.657	$^{+23.407}_{-16.916}$
1390 - 1460	$^{+5.242}_{-14.095}$	$^{+24.854}_{-10.332}$	0.670	$^{+25.410}_{-17.489}$
1460 - 1530	$^{+5.582}_{-14.464}$	$^{+27.170}_{-10.733}$	0.682	$^{+27.746}_{-18.024}$
1530 - 1600	$^{+6.003}_{-14.907}$	$^{+29.741}_{-11.165}$	0.692	$^{+30.349}_{-18.637}$
1600 - 1680	$^{+6.503}_{-15.418}$	$^{+32.855}_{-11.617}$	0.702	$^{+33.500}_{-19.317}$

Table A.7: Theoretical uncertainties (in %) calculated using CT10-NLO PDF set from all sources as well as the total uncertainty, affecting the measurement of cross-section ratio R_{32}, in each bin of $H_{\mathrm{T},2}/2$.

Bin	**Scale**	**PDF**	**NP**	**Total**
300 - 330	$^{+0.038}_{-7.203}$	$^{+2.458}_{-3.463}$	0.822	$^{+2.592}_{-8.035}$
330 - 360	$^{+0.027}_{-6.626}$	$^{+2.317}_{-3.378}$	0.734	$^{+2.431}_{-7.474}$
360 - 390	$^{+0.024}_{-6.449}$	$^{+2.149}_{-3.367}$	0.656	$^{+2.247}_{-7.304}$
390 - 420	$^{+0.084}_{-5.894}$	$^{+2.411}_{-3.383}$	0.586	$^{+2.482}_{-6.821}$
420 - 450	$^{+0.113}_{-5.532}$	$^{+2.345}_{-3.362}$	0.523	$^{+2.405}_{-6.494}$
450 - 480	$^{+0.109}_{-5.409}$	$^{+2.390}_{-3.357}$	0.467	$^{+2.438}_{-6.383}$
480 - 510	$^{+0.073}_{-5.442}$	$^{+2.506}_{-3.327}$	0.416	$^{+2.541}_{-6.392}$
510 - 540	$^{+0.107}_{-5.168}$	$^{+2.559}_{-3.326}$	0.371	$^{+2.588}_{-6.157}$
540 - 570	$^{+0.112}_{-5.010}$	$^{+2.586}_{-3.292}$	0.330	$^{+2.609}_{-6.004}$
570 - 600	$^{+0.163}_{-4.576}$	$^{+2.729}_{-3.292}$	0.292	$^{+2.750}_{-5.645}$
600 - 640	$^{+0.146}_{-4.565}$	$^{+2.824}_{-3.270}$	0.253	$^{+2.839}_{-5.621}$
640 - 680	$^{+0.198}_{-4.163}$	$^{+3.368}_{-3.298}$	0.236	$^{+3.382}_{-5.316}$
680 - 720	$^{+0.155}_{-3.754}$	$^{+2.352}_{-3.247}$	0.227	$^{+2.368}_{-4.968}$
720 - 760	$^{+0.196}_{-3.842}$	$^{+3.267}_{-3.268}$	0.219	$^{+3.280}_{-5.049}$
760 - 800	$^{+0.126}_{-3.523}$	$^{+3.366}_{-3.272}$	0.212	$^{+3.375}_{-4.813}$
800 - 850	$^{+0.110}_{-3.368}$	$^{+3.596}_{-3.261}$	0.206	$^{+3.604}_{-4.693}$
850 - 900	$^{+0.048}_{-3.351}$	$^{+3.909}_{-3.309}$	0.200	$^{+3.915}_{-4.714}$
900 - 950	$^{+0.116}_{-3.504}$	$^{+4.148}_{-3.334}$	0.196	$^{+4.154}_{-4.841}$
950 - 1000	$^{+0.127}_{-3.511}$	$^{+4.300}_{-3.335}$	0.192	$^{+4.306}_{-4.846}$
1000 - 1060	$^{+0.282}_{-3.683}$	$^{+4.604}_{-3.357}$	0.204	$^{+4.617}_{-4.988}$
1060 - 1120	$^{+0.436}_{-3.779}$	$^{+3.079}_{-3.375}$	0.224	$^{+3.118}_{-5.071}$
1120 - 1180	$^{+0.732}_{-3.982}$	$^{+5.430}_{-3.452}$	0.241	$^{+5.485}_{-5.276}$
1180 - 1250	$^{+0.813}_{-4.031}$	$^{+5.835}_{-3.511}$	0.258	$^{+5.897}_{-5.352}$
1250 - 1320	$^{+1.303}_{-4.414}$	$^{+6.626}_{-3.591}$	0.275	$^{+6.759}_{-5.697}$
1320 - 1390	$^{+1.403}_{-4.471}$	$^{+7.036}_{-3.659}$	0.290	$^{+7.180}_{-5.785}$
1390 - 1460	$^{+1.564}_{-4.590}$	$^{+7.657}_{-3.778}$	0.304	$^{+7.822}_{-5.953}$
1460 - 1530	$^{+1.765}_{-4.738}$	$^{+8.438}_{-3.853}$	0.316	$^{+8.626}_{-6.115}$
1530 - 1600	$^{+2.040}_{-4.972}$	$^{+9.306}_{-3.962}$	0.328	$^{+9.532}_{-6.366}$
1600 - 1680	$^{+2.313}_{-5.179}$	$^{+10.381}_{-4.075}$	0.339	$^{+10.641}_{-6.599}$

A.5 Crystal Ball Function

The Crystal Ball function, developed within the Crystal Ball Collaboration, is a probability density function which is often used as a fitting function in high energy physics. This function, described by Eq. A.1, consists of a Gaussian core with separate power-law low-end tails, below a certain threshold.

$$f = N \cdot \begin{cases} e^{-\frac{1}{2}\alpha_L^2} \cdot \left[\left(\frac{\alpha_L}{n_L} \right) \left(\frac{n_L}{\alpha_L} - [\alpha_L + x] \right) \right]^{-n_L}, & x < -\alpha_L \\ e^{-\frac{1}{2}x^2}, & -\alpha_L \leq x \leq \alpha_H \\ e^{-\frac{1}{2}\alpha_H^2} \cdot \left[\left(\frac{\alpha_H}{n_H} \right) \left(\frac{n_H}{\alpha_H} - [\alpha_H + x] \right) \right]^{-n_H}, & x > \alpha_H \end{cases} \tag{A.1}$$

where N is a normalisation factor, α_L and α_H delimit the Gaussian core, which is replaced by a power-law behaviour proportional to $1/n_L$ and $1/n_H$ to the lower and higher side, respectively. The Crystal Ball function itself and its first derivative are continuous.